Cell Stress and Chaperones (2008) 13:447–458
DOI 10.1007/s12192-008-0041-5

ORIGINAL PAPER

Comparison of the effects of 40% oxygen and two atmospheric absolute air pressure conditions on stress-induced premature senescence of normal human diploid fibroblasts

Sangnam Oh · Eunil Lee · Joohyun Lee · Yongchul Lim · Joonhee Kim · Samyong Woo

Received: 24 February 2008 / Revised: 24 March 2008 / Accepted: 24 March 2008 / Published online: 9 May 2008

Abstract The pressure during hyperbaric oxygen treatment may increase oxygen toxicity via an augmented oxygen pressure in the gas. Nevertheless, only a few reports have been published on the effect of cells grown under 2 atmospheric absolute (ATA) pressure. To evaluate the effect of pressure on oxygen toxicity and to study effects in addition to oxygen toxicity, we designed an experiment to compare the effects of normobaric mild hyperoxia (NMH, 40% oxygen) and hyperbaric air condition (HA, air with 2 ATA) on human diploid fibroblasts (HDF) in a hyperbaric incubator. HDFs in both the NMH and the HA condition had a similar oxidative stress response and exhibited premature senescence. To investigate differences in gene profiling in cells grown in the NMH and HA conditions, samples from cells exposed to each condition were applied to microarrays. We found no expression difference in genes related to aging and deoxyribonucleic acid damage, but the expression of genes including cell adhesion, stress response, and transcription were significantly increased in fibroblasts that were responsive to pressure. Among 26 statistically reliable genes, the expression of apoptosis related genes such as ADAM22, Bax, BCL2L14, and UBD, as well as tumor suppressor-related genes like Axin2 and ATF, and also mitogen-activated protein kinase-related genes like mitogen-activated protein kinase kinase kinase 1, histamine receptor, and RAB24, were significantly changed in cells responsive to pressure-induced oxidative stress.

Keywords Hyperbaric oxygenation · Atmospheric pressure · Hyperoxia · Stress-induced premature senescence · Heat shock protein · Microarray · Real time RT-PCR

S. Oh · E. Lee · J. Lee · Y. Lim · J. Kim
Department of Preventive Medicine and Medical Research Center for Environmental Toxico-Genomics and Proteomics, College of Medicine, Korea University, Anam-dong 5ga 126-1, Seongbuk-gu, Seoul 136-705, South Korea

S. Oh · E. Lee · Y. Lim
Cellular and Developmental Biology, Division of Brain Korea 21 Program for Biomedical Science, Korea University, Anam-dong 5ga 126-1, Seongbuk-gu, Seoul 136-705, South Korea

E. Lee (✉) · J. Lee
Postgraduate Studies of Public Health, Graduate School, Korea University, Anam-dong 5ga 126-1, Seongbuk-gu, Seoul 136-705, South Korea
e-mail: eunil@korea.ac.kr

S. Woo
Korea Research Institute of Standards and Science, Yuseng, Deajeon 305-340, Korea

Introduction

Hyperbaric oxygen (HBO_2) therapy has been used for the treatment of hypoxia and prolonged wounds by applying 95% or higher oxygen concentrations intermittently under a greater than ambient pressure. The most frequently preferred pressure range for this treatment is 2–2.5 atmospheric absolute (ATA; Feldmeier 2003; Benedetti et al. 2004). However, HBO_2 also induces strong hyperoxic conditions and increases oxidative stress. These induced events can cause cellular damage by oxidizing lipids, proteins, and deoxyribonucleic acid (DNA), which, in turn, induce apoptosis (Narkowicz et al. 1993). In addition, the expression of heat shock protein (HSP) 70 was significantly

increased in HBO_2-treated cells and animals in which it functioned as a chaperone of oxidative-damaged proteins (Wada et al. 1996; Dennog et al. 1999; Shyu et al. 2004; Yu et al. 2005).

Therefore, many studies have looked at oxidative stress, antioxidant effects, and redox status not only under high concentrations of oxygen tension (Allen and Balin 2003) but also under hyperbaric pressure (Gröger et al. 2005; Oter et al. 2005; Patel et al. 2005).

Most studies on oxygen toxicity in HBO_2 compared the oxidative stress of cells under normoxia (air, 1 ATA), normobaric oxygen (more than 90% oxygen, 1 ATA), and HBO_2 (more than 90% oxygen, more than 1.5 ATA). Hyperbaric conditions have been reported to enhance oxygen toxicity and influence the direction of the negative effects. Oter et al. (2005) reported that since the amount of dissolved oxygen (DO) is directly proportional to the pressure, oxygen toxicity is enhanced due to a pressure-induced increase in DO when cells are exposed to HBO_2.

However, only a few studies have reported on the biological effects other than oxygen toxicity that are caused by hyperbaric pressure. For example, 40 to 120 mmHg pressure promotes DNA synthesis in cultured rat vascular smooth muscle cells (Hishikawa et al. 1994). Therefore, 2 ATA of pressure likely has biological effects in addition to oxygen toxicity. Furthermore, hyperoxic conditions, such as HBO_2 treatment, may not be suited to evaluate the biological effect of 2 ATA of pressure because of the dominant effect of oxygen toxicity.

Normal human diploid fibroblasts (HDFs) undergo oxidative stress-induced premature senescence (SIPS) by their exposure to mild hyperoxia (40% oxygen; von Zglinicki et al. 1995). The expression of hsp70 in WI-38 human fibroblasts was attenuated during aging in vitro (Gutsmann-Conrad et al. 1998). Since the partial pressure of oxygen in normal air with 2 ATA shows an oxygen pressure that is similar to the conditions of 40% oxygen, normal air under 2 ATA may also cause similar oxidative SIPS.

Therefore, stress-induced premature cellular senescence might be an ideal model for the evaluation of the effect of 2 ATA pressure on both oxygen toxicity and other hither-to-uncharacterized biological effects, which need to be elucidated.

The purpose of our present study was to elucidate the effect of 2 ATA pressure on biological processes in normal HDFs because the increase in DO by 2 ATA of air might induce HDF senescence in a manner that is similar to conditions of 40% oxygen. We compared the senescence-associated phenotypes, expression of hsp family, and genomic changes in cells induced by normobaric mild hyperoxia (NMH; 40% oxygen) and hyperbaric air (HA) with 2 ATA.

Materials and methods

Cell line and culture

The human diploid embryonic lung fibroblast cell strains WI-38 (obtained from American Type Culture Collection at the population doubling [PD] level of 25) were maintained in Dulbecco's modified Eagle's medium (Gibco BRL, Grand Island, NY, USA) containing 10% fetal bovine serum (Gibco BRL) as previously described (Hayflick 1965). The subconfluent cells were released from the culture flask and plated at a seeding density of 0.3×10^4 cells per cm^2. Parallel cultures were grown under normoxia (air plus 5% CO_2; pCO_2= 38 mmHg, pO_2=146.566–147.288 mmHg), NMH (40% O_2 plus 5% CO_2; pCO_2=38 mmHg, pO_2=304 mmHg), and HA (2 ATA air plus 5% CO_2; pCO_2=38.228 mmHg, pO_2= 305.9–306.66), which were prepared by mixing air, oxygen, and carbon dioxide at microprocessor-controlled ratios. The inhibition of proliferation was defined as the inability of the culture to reach confluence within 2 weeks.

Hyperbaric pressure chamber

We used a custom-made cell incubator that was specially designed for pressure control. A schematic of the incubator is shown in Fig. 1. In brief, a small cylindrical chamber, which is protected by a Korean (10-2007-0016834) and American (11/942,137) patent, was regulated according to temperature, pressure, humidity, and CO_2. This incubator was equipped to simultaneously control both injection pressure and CO_2 concentration. Injection pressure was measured by a digital readout and a Sensys-pressure

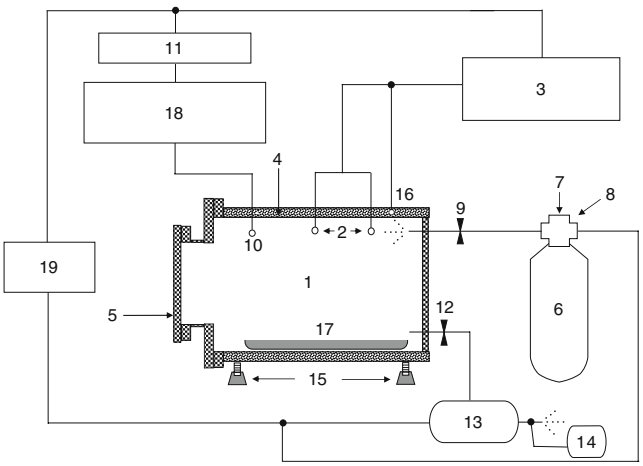

Fig. 1 Schematic of the design for the pressure incubator. Each designation is as follows: *1*, cylindrical pressure chamber; *2* and *16*, thermocouple and sensor; *3*, proportional–integral–derivative controller; *4*, silica jacket; *5*, chamber door; *6*, mixed gas; *7* and *8*, heat and pressure regulator; *9* and *12*, injection or ventilation metering; *11* and *18*, Sensys-pressure transducer and monitoring system; *13*, ventilation pump; *14*, electric CO_2 sensor; *15*, chamber balancer; *17*, water vessel; and *19*, power supply

transducer, while atmospheric CO_2 was measured by an electric sensor that determined the amount of gas present. The chamber contained a thermocouple and a heating element. The heating element was controlled by a proportional–integral–derivative controller.

Determination of pH and dissolved oxygen in the pressure chamber

The pH and DO concentrations in the medium were measured using an expandable ion Analyzer EA920 (Orion Research, Massachusetts, USA) and Sension6 Dissolved Oxygen Electrode (HACH, Loveland, CO, USA), respectively.

Cell morphology and proliferation assay

Morphological changes of cells under each experimental condition were examined by a microscope at ×100 and ×40 magnifications. For cell proliferation assays, the cells were harvested by trypsinization at 24–36-h intervals for a period of 2 weeks. The harvested cells were stained with trypan blue, and the viable cells were counted under a microscope using a hemocytometer. The data are presented as mean± the standard deviation from six replicates.

Senescence-associated β-galactosidase activity

Senescence-associated β-galactosidase (SA-β-GAL) staining has been widely used as a biomarker of cellular senescence in vivo and in vitro (Dimri et al. 1995). To detect SA-β-GAL staining, cells were washed twice in phosphate-buffered saline (PBS), fixed in 3% formaldehyde for 3–5 min at room temperature, and washed again with PBS. Cells were then incubated overnight at 37°C (without CO_2) with freshly prepared SA-β-GAL staining solution (1 mg/ml X-gal, 40 mM citric acid/sodium phosphate; pH 6.0, 5 mM potassium ferrocyanide, 5 mM potassium ferricyanide, 150 mM NaCl, 2 mM $MgCl_2$). All of the blue-stained cells that were found in ten fields (5×10^5 cells) were counted under a microscope with ×100 magnification and expressed as the percentage of positive cells. To avoid cell staining that is caused by cell confluence rather than by proliferative senescence, the assay was performed in subconfluent cultures displaying comparable cell density.

Single-cell gel electrophoresis

To measure DNA damage caused by high oxygen tension, a comet assay was performed according to the method developed by Singh et al. (1988) but with some modifications. In brief, after a fully frosted slide was precoated and spread with 1% agarose as a first layer, cells mixed with low melting agarose (0.5%) were added onto the first layer. The slides were submersed in the lysing solution (2.5 M NaCl, 100 mM ethylenediamine tetraacetic acid [EDTA]-2 Na, 10 mM Tris, and 1% Triton X-100; pH 10) for 2 h. The slides were then placed in an unwinding buffer (1 mM EDTA and 300 mM NaOH; pH>13) for 20 min, and electrophoresis was carried out using the same solution for 20 min at 300 mA (0.8 V/cm). After electrophoresis, the slides were immersed three times in neutralization buffer (0.4 M Tris–HCl, pH 7.2) for 10 min each and were stained with 50 μl of 10 μg/ml ethidium bromide (EtBr). The slides were examined using a Komet 4.0 image analysis system (Kinetic Imaging, Liverpool, UK) fitted with an Olympus BX50 fluorescence microscope equipped with a 515–560-nm excitation filter and a 590-nm barrier filter. For each treatment group, two slides were prepared, and 100 randomly chosen cells (for total 200 cells) were scored, and the parameter of the Olive tail moment (=tail distance×% DNA in tail), where tail distance=center position of tail−center position of the head, was calculated automatically using the Komet 4.0 image analysis system.

Measurement of intracellular reactive oxygen species

Reactive oxygen species (ROS) was measured by a previously described method with some modifications (Ohashi et al. 2002). Treated cells were incubated for 30 min in culture medium containing 30 μM 2′,7′-dichlorofluorescein (DCF) diacetate (DCFH-DA). DCFH-DA penetrates the cells and is first converted to DCFH by cellular esterase and then is oxidized to DCF in the presence of ROS. After incubation with DCFH-DA, the cells were washed twice with PBS and lysed with 10 mM Tris–HCl buffer, pH 7.4, containing 0.5% Tween 20. The lysates were centrifuged at 10,000×g for 10 min to remove cell debris. The DCF fluorescence intensity in the supernatants is an index of intracellular ROS levels, and can be determined by a fluorescence-spectrophotometer using excitation and emission wavelengths at 500 and 536 nm, respectively. The cell number in each sample was counted and used to normalize the fluorescence intensity of DCF.

Telomere length analysis

Genomic DNA was isolated from cells using a DNA extraction kit, G-DEX (intron biotechnology), and used for telomere (terminal restriction fragment [TRF]) length analysis. Genomic DNA (2 μg) was digested with *Hin*fI and *Rsa*I, electrophoresed, and transferred onto a positively charged nylon membrane (Roche, Mannheim, Germany). Hybridization and detection were performed with a chemiluminescent assay kit (TeloTAGGG telomere length assay; Roche, Mannheim, Germany), and the membrane was exposed to Hyperfilm ECL (Amersham). To calculate the TRF, the images were scanned with a densitometer, and the data were analyzed. The mean TRF length was defined as:

$\sum(OD_i)/\sum(OD_i/L_i)$, where OD_i is the densitometer output and L_i the length of the DNA at position i.

Western blot analysis

The proteins resolved on gel were transferred to a polyvinylidene fluoride membrane (Millipore, Bradford, MA, USA), and the membrane was probed with antibodies against cell cycle check point proteins such as p21 (sc-397, Santacruz Biotechnology) and p53 (OP43, Calbiochem) and some HSPs (the antibodies all from Stressgen Biotechnologies), hsp27 (SPA-800), hsp60 (SPA-806), hsp70 (inducible, SPA-810), and hsp90 (SPA-830). Immunoreactivities were detected using an electrochemiluminescence kit (Amersham Biosciences), and quantitative data were obtained using a densitometry (Image system, Kodak)

Microarray analysis

Duplicates of 2-week HDFs under two hyperoxic conditions (NMH and HA) were generated and used for gene expression profiling using the Agilent Whole Human Genome Oligo transcripts. Probe labeling and hybridization were carried out following the manufacturer's specified protocols. Briefly, amplification and labeling of 5 μg of total ribonucleic acid (RNA) was performed using Cy5 to label purified RNA and Cy3 to label the reference RNA (Stratagene UHR). Hybridization was performed for 16 h at 60°C, and the arrays were scanned on an Agilent DNA microarray scanner. Scanned images were analyzed with a Micro Array Scanner G2505B (Agilent Technologies, Santa Clara, CA, USA) to obtain gene expression ratios.

Fluorescence real-time quantitative reverse transcriptase polymerase chain reaction

Some of the genes identified from the microarray experiment were validated by fluorescence real-time quantitative reverse transcriptase polymerase chain reaction (PCR). Real-time quantitative PCR was performed using the ABI Prism 7900 Sequence Detection System (PE Applied Biosystems). The fluorescence emission from each sample was collected by a charge-coupled device camera, and the quantitative data were analyzed using the Sequence Detection System software (SDS version 2.0, PE Applied Biosystems).

Primer sequence

The following were the sequences of the primers used in the study:

KIFAP3 (139 bp): ACC AGT TGG CAT TCT TGG AC/ACC CAA CCC ACA CAG ATT TC

BAX (100 bp): GAC GGC CTC CTC TCC TAC TT/ CCA TCT TCT TCC AGA TGG TGA

ATF3 (140 bp): TCG GAG AAG CTG GAA AGT GT/ TCT GGA GTC CTC CCA TTC TG

Statistical analysis

Most experiments were conducted at least in triplicate. The effects of each treatment were analyzed by analysis of variance, followed by Duncan's test using the SAS software package (Version 9.1; SAS, Cary, NC, USA). The level of significance was defined at $p<0.05$. The statistical analysis of gene values from the microarray was performed by GeneSpring GX 7.3.1 (Agilent Technologies).

Results

Exposing HDF cells to HA and NMH increases oxidative stress and DNA damage

Although the pH values of the culture media were not significantly different among the three culture conditions (7.2–7.3), DO_2 levels in both HA and NMH exposure conditions were significantly increased by twofold more than when grown under normoxia conditions because of the augmented partial oxygen in gas (Fig. 2). To study whether there were differences in the intracellular oxidative stress level between the HA- and NMH-treated cells, we fluorospectrometrically measured the amount of deacetylated DCFH-DA to assay the concentration of intracellular hydrogen peroxide in the cells. As seen in Fig. 3, the relative DCF intensities in cells treated either with HA or NMH for 4 and 14 days were very similar. These intensities were 3 and 4.5 times higher than the values from normoxic cells at 33 PDs (both groups, $p<0.001$). The intracellular hydrogen peroxide levels of HA- and NMH-treated cells were similar to replicatively senescent cells at 58 PDs.

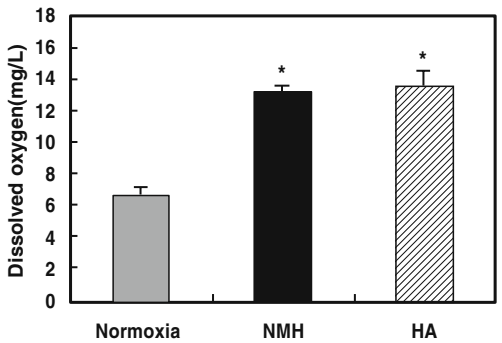

Fig. 2 The elevated levels of DO in the culture medium exposed to NMH (*black bar*) or HA (*dashed bar*) was statistically significant. The DO was increased twofold in proportion to the pressure, according to Henry's law

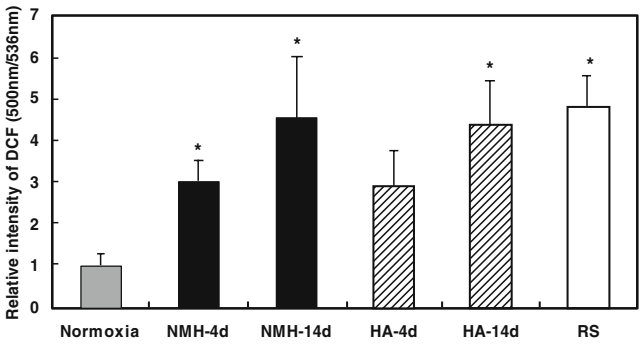

Fig. 3 Relative quantities of hydrogen peroxide in HDF under NMH or HA were measured at 4 and 14 days. The intensity of DCF was measured fluorospectrometrically and each intensity value was normalized by normoxic data (*gray bar*). The levels under HA (*dashed bar*) and NMH (*black bar*) increased significantly at 4 and 14 days, and their levels at 14 days were similar to those of replicative senescent cells (*white bar*)

Therefore, the hyperoxic condition induced by HA is similar to the condition induced by NMH with regard to the surrounding or intracellular oxygen toxicity and oxidative stress.

DNA damage in the cells exposed to both HA and NMH were also similar, with these cells showing higher Olive tail moment values than control cells (Fig. 4a). In contrast, the DNA damage of control cells under the condition of normoxia showed lower values. Furthermore, these values for DNA damage in the control cells did not change as the cells grew. The extent of DNA damage, as measured by percent DNA in the tail, revealed similar results as those measured by the Olive tail moment. In addition, the distribution of cells with highly damaged DNA exposed to HA and NMH was higher than the distribution of cells grown under the condition of normoxia (Fig. 4b).

Cell proliferation is almost inhibited by exposure to both HA and NMH

After 1 week of exposure to either HA or NMH, cells no longer divided (Fig. 5). As shown in Fig. 5b, when compared to control cells, PDs were significantly decreased in cells responsive to HA and NMH. This effect did not differ in cells treated with either of the two hyperoxic conditions.

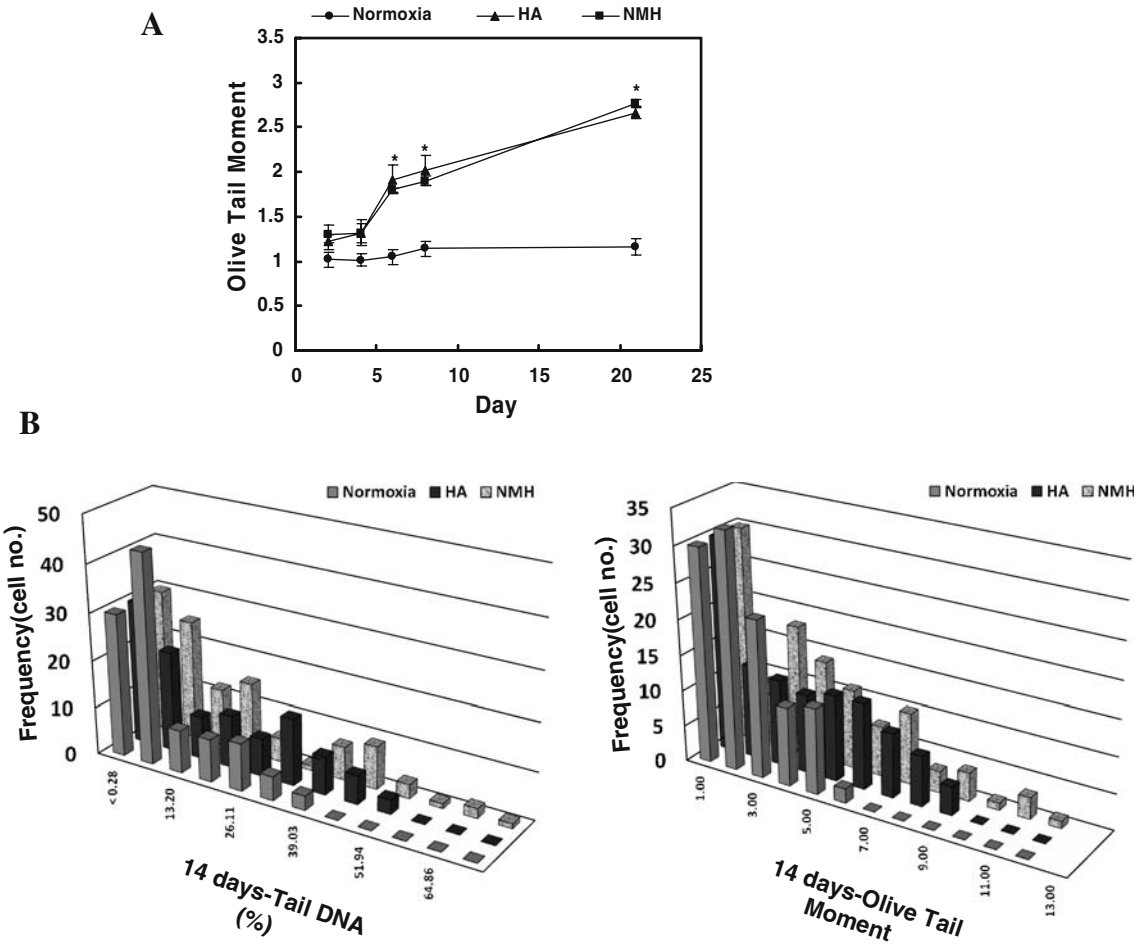

Fig. 4 The time dependence of HDF exposed to NMH or HA, as measured by the comet assay. The comet value of HDF exposed to HA (*triangle*) and NMH (*square*) increased to a significantly high value, in contrast to HDF exposed to normoxia (*circle*). Each point shows that the mean Olive tail moment±the SEM from at least 110 comets measured in each of three experiments

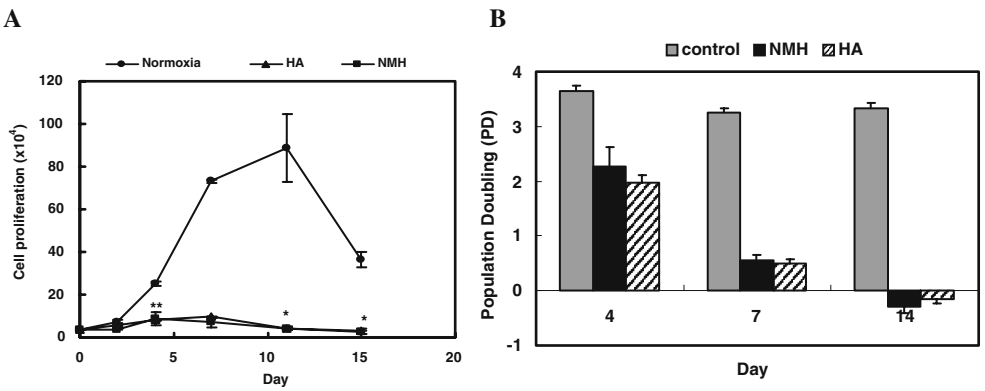

Fig. 5 The inhibitory effects of HA or NMH on the population growth of HDF. HDF were stained with trypan blue, and viable cells were counted at 24–36-h intervals for 2 weeks. Data are presented as the mean± standard deviation from six replicates

Cells exposed to HA or NMH have increased SA-β-GAL activity but not telomere shortening

Both HA- and NMH-treated cells exhibited the typical senescent cell morphology, such as cell enlargement, a reduced cytoplasm-to-nuclear ratio, saturation density, and increased SA-B-GAL activity, after 7 days of culture (Fig. 6). After this time point, the cells gradually displayed the characteristics of replicatively senescent cells in a time-dependent manner. About 50% blue-stained cells have been shown after 14 days of culture under both conditions. No differences were observed between HA- and NMH-treated cells with regard to the percentage of senescent cells, percentage of senescent morphologies, and the high density of positive blue-stained cells. We also performed a telomere length assay to elucidate whether telomere shortening occurred during the induction of premature senescence by HA. We observed that telomere shortening did not happen when the cells were exposed to both HA and NMH (Fig. 7).

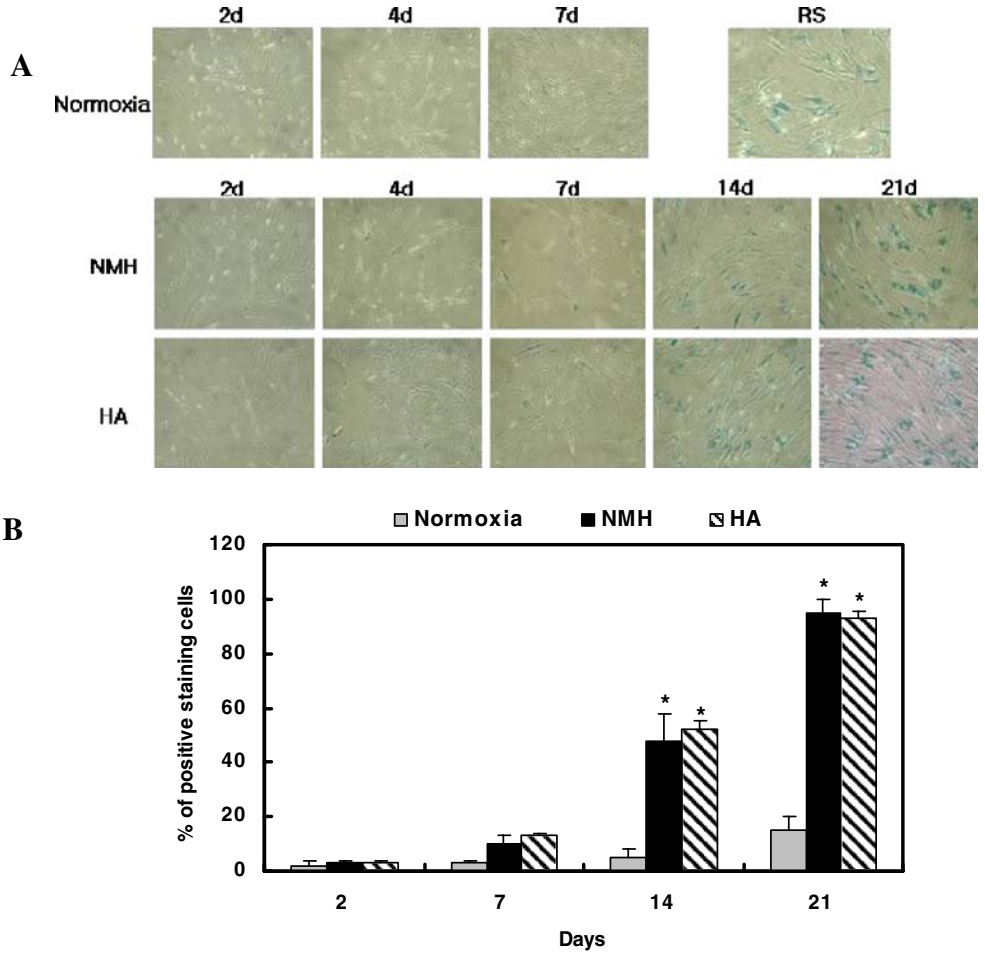

Fig. 6 Change of morphology and SA-b-gal staining in HDF as induced by exposure to HA and/or NMH. **a** The microscopic images of HDF in response to HA or NMH at ×40 magnification. **b** The percentage of positive blue stained cells out of the total number of observed cells was calculated and diagramed

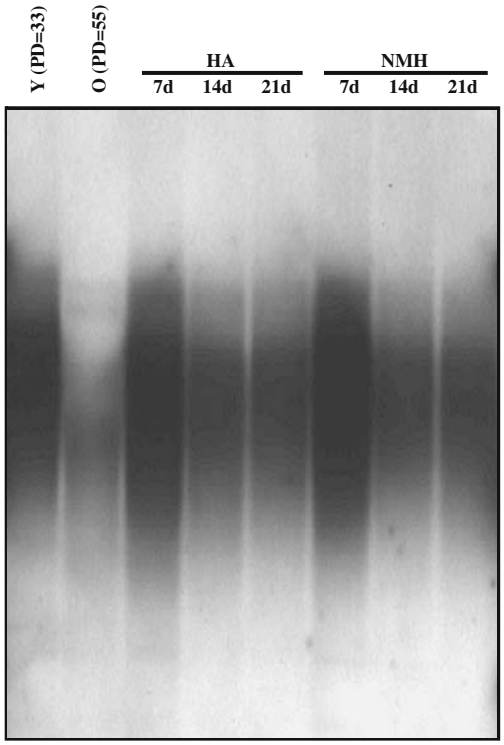

Fig. 7 Nonsignificantly changed telomere lengths in HDF exposed to HA or NMH for 1, 2, or 3 weeks. Two micrograms of each sample was loaded and applied to a TeloTAGGG probe

Expression of heat shock proteins and cell cycle check point proteins in HA- and NMH-treated cells

We investigated the differential expression of hsp27, hsp60, hsp70, and hsp90 in cells treated with HA or NMH at day 14 when cells showed a significant senescence phenotype (Fig. 6). Basal levels of hsp27/70 were significantly decreased, and hsp60 was slightly increased in HA- or NMH-treated cells compared with control cells (Fig. 8a); however, there were no significant differences in cultured cells in response to each hyperoxic condition. With regard to cell cycle check points, both p21 and p53 were upregulated in cells exposed to HA or NMH (Fig. 8b).

Gene expression analysis of HA- and NMH-treated cells by microarray and Real-time PCR

We used an array that contained 44,000 probe sets from whole human genes for the target hybridization. The distribution profile of all expressed genes in HA-treated cells consisted of about 0.091% upregulated genes and 0.034% downregulated genes. The percentage of differentially expressed genes was very small over the entire human genome. These results suggested that the effect on messenger RNA (mRNA) transcription was similar in HA- and NMH-treated cells. Of the differentially expressed genes, a total of 26 genes were statistically reliable, including 22 upregulated genes and 4 downregulated genes

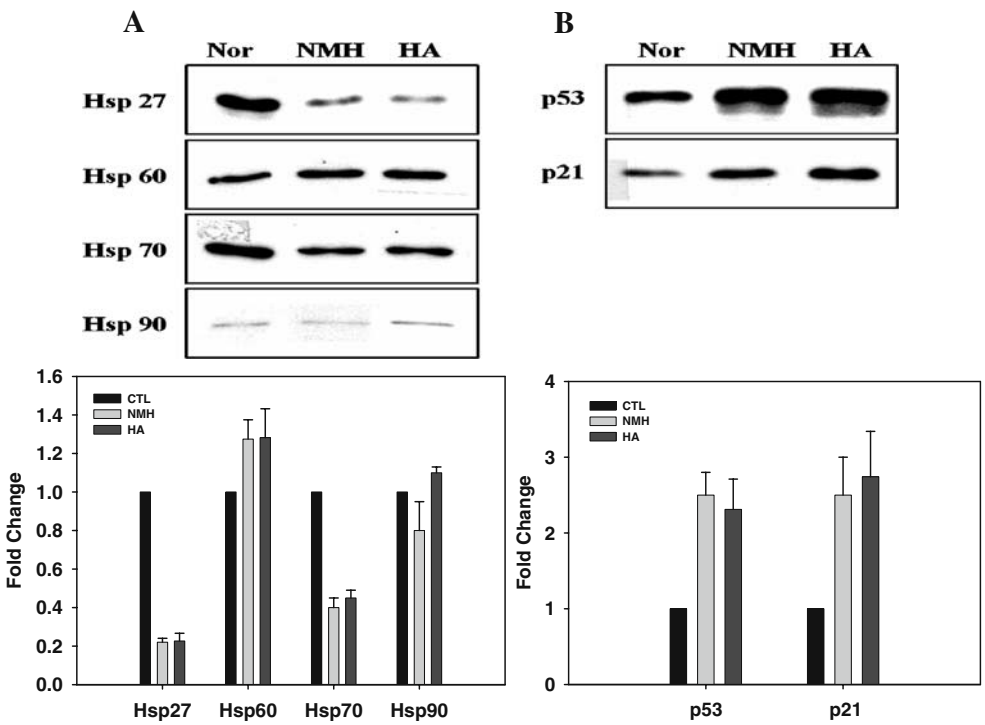

Fig. 8 The levels of HSPs (**a**), p21, and p53 (**b**) in HDF in response to HA or NMH by Western blot analysis. The densities of each protein expression were analyzed by EL100 Image system and corrected by the densities of β-actin

(Fig. 9). The genes associated with cell adhesion, cytoskeleton, and antibacterial response were significantly increased in fibroblasts that responded to pressure. Only HA-exposed cells exhibited an increase in cell adhesion molecules, like ADAM metallopeptidase domain 22, apoptosis related genes, like Bax and BCL2-like 14, antibacterial stress-related genes, like musin and defensin, mitogen-activated protein kinase (MAPK)-related genes, like mitogen-activated protein kinase kinase kinase 1 (MEKK1) and histamine receptor (GPCR). To confirm the expression of several mRNAs, we performed fluorescence real-time quantitative PCR (Fig. 10)

These results suggested that 2 ATA of pressure increases oxidative stress to cause the SIPS of cells, which is similar to the conditions initiated when cells are exposed to 1 ATA hyperoxic (40%) air. However, 2 ATA of pressure may have a different significant biological effect on cell adhesion, the cytoskeleton, the stress response, and transcription.

Discussion

Although HBO_2 therapy is a useful remedy that supplies sufficient oxygen to tissues and organs, this therapy also increases oxidative stress, thus causing cellular damage and death (Narkowicz et al. 1993). The toxicity of high concentrations of oxygen has been shown in numerous whole-animal studies and cell culture models (Halliwell 1981; Davies 1999). Furthermore, HBO_2 treatment increases oxygen toxicity, such as seizure activity and death with severe pulmonary edema (Pablos et al. 1997). The exposure of keratinocytes to normobaric 90% oxygen induced partial G2/M arrest, and a small population of cells underwent apoptosis, but in response to hyperbaric 90% oxygen, the cell growth was substantially arrested, and the number of apoptotic cells increased by more than sixfold (Patel et al. 2005). In vivo electron paramagnetic

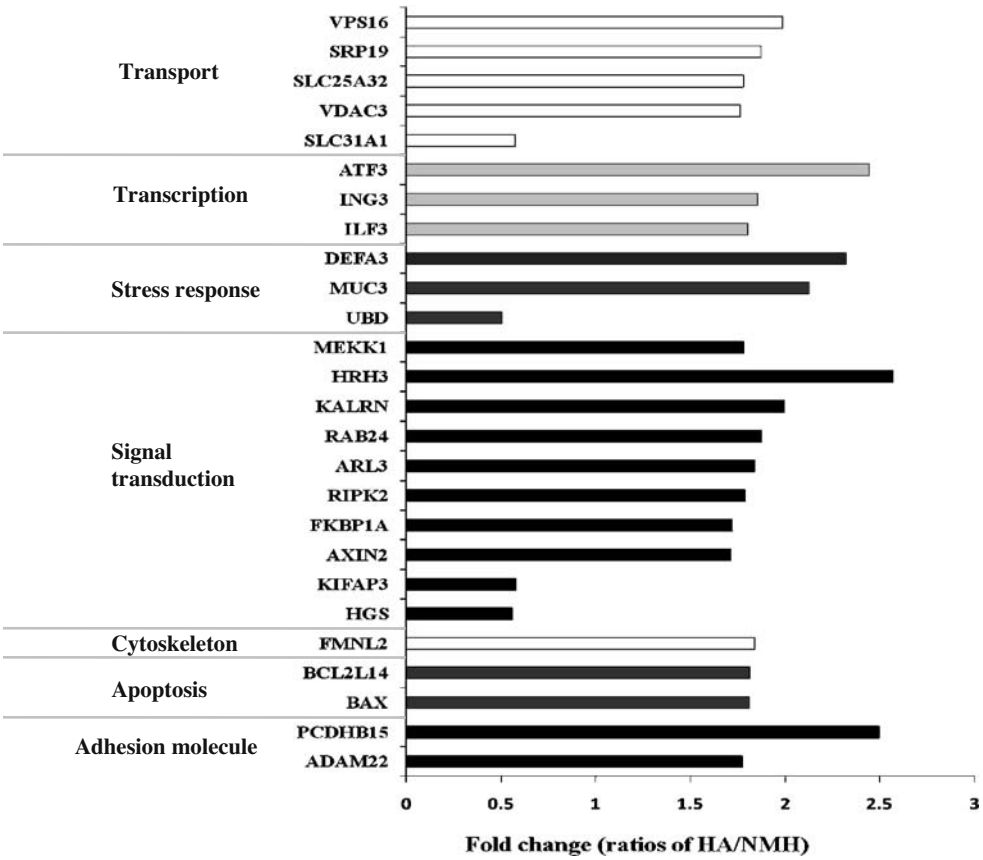

Fig. 9 Up- and downregulation of genes in HA-treated cells for 14 days. Each function has several genes that have been produced by replicate analysis with duplication ($p<0.05$). *UBD* indicates ubiquitin D (FAT10); *HGS*, hepatocyte growth factor-regulated tyrosine kinase substrate; *SLC31A1*, solute carrier family 31 (copper transporters); *KIFAP3*, kinesin-associated protein 3; *AXIN2*, axin 2 (conductin, axil); *FKBP1A*, FK506-binding protein 1A (12 kDa); *VDAC3*, voltage-dependent anion channel 3; *ADAM22*, ADAM metallopeptidase domain 22; *MEKK1*, mitogen-activated protein kinase kinase kinase 1; *SLC25A32*, solute carrier family 25, member 32; *RIPK2*, receptor-interacting serine–threonine kinase 2; *ILF3*, interleukin enhancer binding factor 3 (90 kDa); *BAX*, BCL2-associated X protein; *BCL2L14*, BCL2-like 14 (apoptosis facilitator), *FMNL2*, formin-like 2; *ARL3*, ADP-ribosylation factor-like 3; *ING3*, inhibitor of growth family, member 3, *SRP19*, signal recognition particle 19 kDa, RAB24, member RAS oncogene family; *VPS16*, vacuolar protein sorting 16 homolog; *KALRN*, kalirin, RhoGEF kinase; *MUC3*, mucin-3; *DEFA3*, defensin, alpha 3; *ATF3*, activating transcription factor 3; *PCDHB15*, protocadherin beta 15; *HRH3*, histamine receptor H3

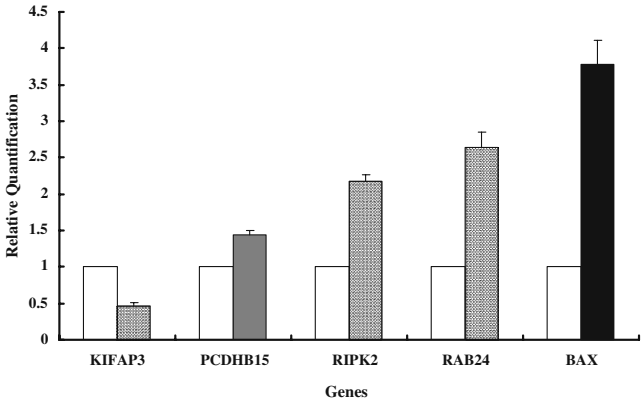

Fig. 10 Real-time reverse transcriptase PCR assay validation for a subset (PCDHB15, RAB24, BAX, RIPK2, and KIFAP3) of altered genes in HDF treated with HA compared to NMH-treated cells as a control. The data shown are the relative quantifications for each target gene compared to the GAPDH control gene in the HA- or NMH-treated cells

resonance spectroscopy imaging in mice exposed to HBO_2 revealed a shift in the whole-body redox status toward oxidation (Patel et al. 2005). Therefore, these studies imply that using pressure with high oxygen for therapy has a negative effect in vivo and in vitro and suggests that a lower pressure should be applied. In fact, even more normobaric topical oxygen therapy has been suggested as an improvement to HBO_2 treatment (Oter et al. 2005).

The effects of hyperbaric pressure have focused mainly on oxygen toxicity, but few research studies have attempted to elucidate the biological effects of 2 ATA pressure, which has predominately been used in HBO_2. Depending on the cell type, pressures less than 2 ATA had diverse effects, including accelerated aging (Pablos et al. 1997). These results suggested that this aging effect was directly related to the level of pressure. Oxidative SIPS caused by HDF has been reported, and mild hyperoxia (40% oxygen) has been shown to induce premature senescence in normal HDFs (Chen and Ames 1994; von Zglinicki et al. 1995; Chen 2000; Toussaint et al. 2000). HA (air with 2 ATA) may induce premature senescence because of high oxygen pressure and other biological effects.

In our study, the partial pressure of oxygen in HA and the air that is 40% oxygen should be similar, and thus the oxidative stress and the stress-induced senescence features in cells treated with HDF were almost the same under conditions of NMH (40% oxygen) and HA (21% oxygen) (Fig. 2~6). DO levels and intracellular H_2O_2 were significantly increased by more than 2-fold, compared with cells exposed to normoxia, because of the augmented partial oxygen (Fig. 2). Moreover, we showed that the DNA damage to HDFs under NMH and HA treatments depended on the duration and the manner of exposure (Fig. 3). Both conditions induced typical cellular senescence phenomena such as the inhibition of cell proliferation, cell growth arrest, senescence-like-cell morphology, enhanced SA-B-GAL activity with no significant difference.

Telomere length shortening did not occur under either HA or NMH. These results suggest that HA and NMH induced the same oxidative stress and SIPS via similar

Table 1 The significantly changed expression of genes that have functions of apoptosis and tumor were summarized

General function	Description	Gene	Significant role	Change
Adhesion molecule	ADAM metallopeptidase domain 22	ADAM22	Inhibition of cell proliferation (D'Abaco et al. 2006), migration and invasion (Kang et al. 2000), induction of apoptosis (Chung et al. 2003)	Increase
Apoptosis	BCL2-associated X protein	BAX	Pro-apoptotic proteins (Adams and Cory 1998),	Increase
	BCL2-like 14 (apoptosis facilitator)	BCL2L14	mitochondrial dysfunction (Gross et al. 1998)	Increase
Signal transduction	Axin 2 (conductin, axil)	AXIN2	Negative regulator of Wnt/β-catenin signaling (Kikuchi 1999; Liu et al. 2000; Hughes and Brady 2005a), Tumor suppressor (Hughes and Brady 2005b)	Increase
	Member RAS oncogene family	RAB24	Triggering the MAPK pathway and ultimately	Increase
	Kalirin, RhoGEF kinase	KALRN	induction of the expression of factors that	Increase
	Histamine receptor H3	HRH3	survival or death (Davis 1993)	Increase
	MEKK1	MEKK1		Increase
Stress response	Ubiquitin D (FAT10)	UBD	Negative regulator of p53 (Ren et al. 2006; Zhang et al. 2006), increased sensitivity of apoptotic cell death (Canaan et al. 2006)	Decrease
	Mucin-3	MUC3	Inflammatory, immune response and wound (Hughes and Brady 2005b).	Increase
	Defensin, alpha 3	DEFA3		Increase
Transcription	Activating transcription factor 3	ATF3	Maintaining DNA integrity and protecting against cell transformation (Yan et al. 2005)	Increase

oxygen toxicities, because both conditions have the same oxygen partial pressure.

Moreover, the expressions of proteins involved in heat shock and cell cycle check points were not significantly different between the two hyperoxic conditions. It is interesting to note that hsp27 was dramatically decreased under both conditions. A recent study reported that elevated levels of hsp27 protected human mammary epithelial cells from doxorubicin. This protection was associated with suppression of doxorubicin-induced senescence, whereby Hsp27 inhibited p53-mediated induction of p21, the major regulator of the senescence program (O'Callaghan-Sunol et al. 2007). In other words, the common characteristic of cells treated with HA or NMH may be that senescence-like phenotypes are induced by Hsp27 downregulation associated with the activation of the p53 pathway and the induction of p21. An attenuated basal level of hsp70 has also been shown in fibroblasts from old donors compared to young donors (Gutsmann-Conrad et al. 1998). An increase in HSP60 protein levels has also been reported to be associated with a cell cycle slowdown; thus, it may play a role in cell cycle progression related to cellular senescence (Di Felice et al. 2005). In addition, hsp60 expression increased in response to oxidative and cellular stress (Calabrese et al. 2007). The relationships among various stress response proteins under stressful conditions that trigger premature senescence have not yet been elucidated.

Although we found no significantly different effects on oxidative stress, DNA damage, and SIPS of the cells treated with HA and NMH, the genomic profiles of these cell populations were different. When cells underwent pressure stress with hyperoxia, genes associated with adhesion, apoptosis, cytoskeleton, and signal transduction were increased. Cellular adhesion plays an important role in a variety of biological processes, including embryonic development and in tumor cell invasion and metastasis. Among the changed expression of genes, the following genes that have a significant function such as apoptosis and tumor were summarized as a table (Table 1). The ADAM22 gene that contains disintegrin-like and metalloproteinase-like domains that potentially have cell adhesion and protease activities (Blobel 2002; Seals and Courtneidge 2003) was increased in response to the treatment of HA compared to normoxia. Its low expression has been suggested to act as a marker for tumor progression in glioma (D'Abaco et al. 2006). Some apoptosis-related genes, such as the apoptotic marker Bax (BCL2-associated X protein) and the apoptotic activator BCL2-like 14, which can trigger a mitochondrial dysfunction (Gross et al. 1998), were increased in the HA-treated cells. In addition, tumor suppressor genes like Axin2 and activating transcription factor (ATF3) under HA were induced higher than NMH. The genes involving signal transduction such as MEKK1, GPCR, receptor-interacting serine–threonine kinase 2, and RAS oncogene family, which can be trigger the MAPK pathway, were increased. As bacterial stress-responsive genes, defensin and mucin were also shown to be increased in HA-treated cells. However, a decrease in ubiquitin D (FAT10), a member of the ubiquitin-like modifier family of proteins, which is also related to apoptosis as a negative regulator of p53, was observed. In brief, genomic analysis showed that the genes that induced apoptosis and suppressed tumorigenesis and the MAP kinase-including genes were all found in HA-treated cells. Though the oxidative stress response was very similar between the cells exposed to HA and NMH conditions expected from the premature senescence-like phenotype, the genomic changes that reflected the whole effect of pressure were different.

In the earlier studies, there were some reports that neonatal fibroblasts grown under elevated static pressure demonstrated inhibited growth rates, increased fibronectin production (Healey et al. 2003), and senescent morphologies in an in vitro model (Stanley et al. 2005). On the other hand, cardiac growth (hypertrophy of cardiac muscle cell and nonmuscle cell) in rat can be induced by pressure (Dowell and McManus 1978; Teiger et al. 1996). The overloading of static pressure (30–90 mmHg) can enhance DNA synthesis and matrix synthesis (Mattana and Singhal 1995) through MAPK activation (Kawata et al. 1998) in mesangial cells.

Our study suggests that mechanical 2 ATA pressure induces similar SIPS in human fibroblasts like SIPS via 40% oxygen toxicity. It is nteresting to note that we found no changes in the gene or protein expression of p53 and heat shock genes related to cell stress, in response to either HA and NMH, which both trigger a senescence-like phenotype. However, the 2-ATA pressure stimulus could affect important biological processes such as apoptosis and tumorigenesis. Future study is warranted to elucidate the molecular mechanisms of these processes; such studies should examine the variety of extracellular ligands, their interaction with cell membrane receptors, and subsequent downstream signaling cascades resulting in oxygen toxicity correlated with pressure.

Acknowledgments This research was supported by the grant from the Medical Research Center for Environmental Toxicogenomic and Proteomics (R13-2003-016-00000-0), funded by Korea Science and Engineering Foundation and Ministry of Science and Technology.

References

Adams JM, Cory S (1998) The Bcl-2 protein family: arbiters of cell survival. Science 281:1322–1326

Allen RG, Balin AK (2003) Effects of oxygen on the antioxidant responses of normal and transformed cells. Exp Cell Res 289:307–316

Benedetti S, Lamorgese A, Piersantelli M, Pagliarani S, Benvenuti F, Canestrari F (2004) Oxidative stress and antioxidant status in patients undergoing prolonged exposure to hyperbaric oxygen. Clin Biochem 37:312–317

Blobel CP (2002) Functional and biochemical characterization of ADAMs and their predicted role in protein ectodomain shedding. Inflamm Res 51:83–84

Calabrese V, Mancuso C, Sapienza M et al (2007) Oxidative stress and cellular stress response in diabetic nephropathy. Cell Stress Chaperones 12:299–306

Canaan A, Yu X, Booth CJ et al (2006) FAT10/ diubiquitin-like protein-deficient mice exhibit minimal phenotypic differences. Mol Cell Biol 26:5180–5189

Chen QM (2000) Replicative senescence and oxidant-induced premature senescence. Beyond the control of cell cycle checkpoints. Ann NY Acad Sci 908:111–125

Chen Q, Ames BN (1994) Senescence-like growth arrest induced by hydrogen peroxide in human diploid fibroblast F65 cells. Proc Natl Acad Sci USA 91:4130–4134

Chung KH, Kim SH, Han KY et al (2003) Inhibitory effect of salmosin, a Korean snake venom-derived disintegrin, on the integrin alphav-mediated proliferation of SK-Mel-2 human melanoma cells. J Pharm Pharmacol 55:1577–1582

D'Abaco GM, Ng K, Paradiso L, Godde NJ, Kaye A, Novak U (2006) ADAM22, expressed in normal brain but not in high-grade gliomas, inhibits cellular proliferation via the disintegrin domain. Neurosurgery 58:179–186

Davies KJ (1999) The broad spectrum of responses to oxidants in proliferating cells: a new paradigm for oxidative stress. IUBMB Life 48:41–47

Davis RJ (1993) The mitogen-activated protein kinase signal transduction pathway. J Biol Chem 268:14553–14556

Dennog C, Radermacher P, Barnett YA, Speit G (1999) Antioxidant status in humans after exposure to hyperbaric oxygen. Mutat Res 428:83–89

Di Felice V, Ardizzone N, Marcianò V, Bartolotta T, Cappello F, Farina F, Zummo G (2005) Senescence-associated HSP60 expression in normal human skin fibroblasts. Anat Rec A Discov Mol Cell Evol Biol 284:446–453

Dimri GP, Lee X, Basile G et al (1995) A biomarker that identifies senescent human cells in culture and in aging skin in vivo. Proc Natl Acad Sci USA 92:9363–9367

Dowell RT, McManus RE 3rd (1978) Pressure-induced cardiac enlargement in neonatal and adult rats. Left ventricular functional characteristics and evidence of cardiac muscle cell proliferation in the neonate. Circ Res 42:303–310

Feldmeier JJ (2003) Hyperbaric oxygen 2003: indications and results. The Hyperbaric Oxygen Therapy Committee Report UHMS, Undersea and Hyperbaric Medical Society, Kensington, MD, pp 87–100

Gröger M, Speit G, Radermacher P, Muth CM (2005) Interaction of hyperbaric oxygen, nitric oxide, and heme oxygenase on DNA strand breaks in vivo. Mutat Res 572:167–172

Gross A, Jockel J, Wei MC, Korsmeyer SJ (1998) Enforced dimerization of BAX results in its translocation, mitochondrial dysfunction and apoptosis. EMBO J 17:3878–3885

Gutsmann-Conrad A, Heydari AR, You S, Richardson A (1998) The expression of heat shock protein 70 decreases with cellular senescence in vitro and in cells derived from young and old human subjects. Exp Cell Res 241:404–413

Halliwell B (1981) Free radicals, oxygen toxicity and aging. In: Sohal RS (ed) Age pigments. North-Holland Biomedical, Amsterdam, pp 1–6

Hayflick L (1965) The limited in vitro lifetime of human diploid cell strains. Exp Cell Res 37:614–636

Healey C, Forgione P, Lounsbury KM, Corrow K, Osler T, Ricci MA, Stanley A (2003) A new in vitro model of venous hypertension: the effect of pressure on dermal fibroblasts. J Vasc Surg 38:1099–1105

Hishikawa K, Nakaki T, Marumo T, Hayashi M, Suzuki H, Kato R, Saruta T (1994) Pressure promotes DNA synthesis in rat cultured vascular smooth muscle cells. J Clin Invest 93:1975–1980

Hughes TA, Brady HJ (2005a) Cross-talk between pRb/E2F and Wnt/beta-catenin pathways: E2F1 induces axin2 leading to repression of Wnt signalling and to increased cell death. Exp Cell Res 303:32–46

Hughes TA, Brady HJ (2005b) Expression of axin2 is regulated by the alternative 5¢-untranslated regions of its mRNA. J Biol Chem 280:8581–8588

Kang IC, Kim DS, Jang Y, Chung KH (2000) Suppressive mechanism of salmosin, a novel disintegrin in B16 melanoma cell metastasis. Biochem Biophys Res Commun 275:169–173

Kawata Y, Mizukami Y, Fujil Z, Sakumura T, Yoshida K, Matsuzaki M (1998) Applied pressure enhances cell proliferation through mitogen-activated protein kinase activation in mesangial cells. J Biol Chem 273:16905–16912

Kikuchi A (1999) Modulation of Wnt signaling by Axin and Axil. Cytokine Growth Factor Rev 10:255–265

Liu W, Dong X, Mai M et al (2000) Mutations in AXIN2 cause colorectal cancer with defective mismatch repair by activating beta-catenin/TCF signaling. Nat Genet 26:146–147

Mattana J, Singhal PC (1995) Applied pressure modulates mesangial cell proliferation and matrix synthesis. Am J Hypertens 8:1112–1120

Narkowicz CK, Vial JH, McCartney PW (1993) Hyperbaric oxygen therapy increases free radical levels in the blood of humans. Free Radic Res Commun 19:71–80

O'Callaghan-Sunol C, Gabai VL, Sherman MY (2007) Hsp27 modulates p53 signaling and suppresses cellular senescence. Cancer Res 67:11779–11788

Ohashi T, Mizutani A, Murakami A, Kojo S, Ishii T, Taketani S (2002) Rapid oxidation of dichlorodihydrofluorescin with heme and hemoproteins: formation of the fluorescein is independent of the generation of reactive oxygen species. FEBS Lett 511:21–27

Oter S, Korkmaz A, Topal T, Ozcan O, Sadir S, Ozler M, Ogur R, Bilgic H (2005) Correlation between hyperbaric oxygen exposure pressures and oxidative parameters in rat lung, brain, and erythrocytes. Clin Biochem 38:706–711

Pablos MI, Reiter RJ, Chuang JI et al (1997) Acutely administered melatonin reduces oxidative damage in lung and brain induced by hyperbaric oxygen. J Appl Physiol 83:354–358

Patel V, Chivukula IV, Roy S et al (2005) Oxygen: from the benefits of inducing VEGF expression to managing the risk of hyperbaric stress. Antioxid Redox Signal 7:1377–1387

Ren J, Kan A, Leong SH, Ooi LL, Jeang KT, Chong SS, Kon OL, Lee CG (2006) FAT10 plays a role in the regulation of chromosomal stability. J Biol Chem 281:11413–11421

Seals DF, Courtneidge SA (2003) The ADAMs family of metalloproteases: multidomain proteins with multiple functions. Genes Dev 17:7–30

Shyu WC, Lin SZ, Saeki K et al (2004) Hyperbaric oxygen enhances the expression of prion protein and heat shock protein 70 in a mouse neuroblastoma cell line. Cell Mol Neurobiol 24:257–268

Singh NP, McCoy MT, Tice RR, Schneider EL (1988) A simple technique for quantitation of low levels of DNA damage in individual cells. Exp Cell Res 175:184–191

Stanley AC, Lounsbury KM, Corrow K, Callas PW, Zhar R, Howe AK, Ricci MA (2005) Pressure elevation slows the fibroblast response to wound healing. J Vasc Surg 42:546–551

Teiger E, Than VD, Richard L et al (1996) Apoptosis in pressure overload-induced heart hypertrophy in the rat. J Clin Invest 97:2891–2897

Toussaint O, Medrano EE, von Zglinicki T (2000) Cellular and molecular mechanisms of stress-induced premature senescence (SIPS) of human diploid fibroblasts and melanocytes. Exp Gerontol 35:927–945

von Zglinicki T, Saretzki G, Döcke W, Lotze C (1995) Mild hyperoxia shortens telomeres and inhibits proliferation of fibroblasts: a model for senescence? Exp Cell Res 220:186–193

Wada K, Ito M, Miyazawa T, Katoh H, Nawashiro H, Shima K, Chigasaki H (1996) Repeated hyperbaric oxygen induces ischemic tolerance in gerbil hippocampus. Brain Res 740:15–20

Yan C, Lu D, Hai T, Boyd DD (2005) Activating transcription factor 3, a stress sensor, activates p53 by blocking its ubiquitination. EMBO J 24:2425–2435

Yu SY, Chiu JH, Yang SD, Yu HY, Hsieh CC, Chen PJ, Lui WY, Wu CW (2005) Preconditioned hyperbaric oxygenation protects the liver against ischemia-reperfusion injury in rats. J Surg Res 128:28–36

Zhang DW, Jeang KT, Lee CG (2006) p53 negatively regulates the expression of FAT10, a gene upregulated in various cancers. Oncogene 25:2318–2327